Synthesis, Structure, and Hg 2+ –Ion–Sensing Properties of Stable Calixazasmaragdyrins

3 AUTHORS, INCLUDING:

Tamal Chatterjee
Indian Institute of Technology Bombay
15 PUBLICATIONS   22 CITATIONS

SEE PROFILE

Sivaiah Areti
Indian Institute of Technology Bombay
8 PUBLICATIONS   7 CITATIONS

SEE PROFILE

Synthesis, Structure, and Hg²⁺-Ion-Sensing Properties of Stable Calixazasmaragdyrins

Tamal Chatterjee, Sivaiah Areti, and Mangalampalli Ravikanth*

Department of Chemistry, Indian Institute of Technology Bombay, Mumbai 400 076, India

S *Supporting Information*

ABSTRACT: The first stable calixazasmaragdyrins containing two *meso*-sp² and one *meso*-sp³ carbon atoms were synthesized by [3 + 2] condensation of 2,2′-(1-methylethylidene)bis-(pyrrole) and 5,10-diaryltripyrromethane under trifluoroacetic acid catalyzed conditions. The macrocycles were confirmed by high-resolution mass spectrometry, and the molecular structures were deduced by detailed 1D and 2D NMR spectroscopy. The single-crystal structural analysis showed the highly strained and distorted nature of a calixazasmaragdyrin macrocycle. The presence of the one *meso*-sp³ carbon center induces sufficient flexibility into the macrocycle, which, in turn, helps with the stability of the calixazasmaragdyrin macrocycle. The calixazasmargdyrins showed one broad absorption band at ~425 nm and an ill-defined band at ~685 nm. The electrochemical studies revealed that the calixazasmaragdyrins are not stable under redox conditions. Because the calixazasmargdyrin macrocycle possesses five pyrrole rings with three ionizable inner NH protons, we investigated anion and cation sensing properties of calixazasmargdyrins. Our studies revealed that the calixazasmaragdyrins do not show any sensing behavior toward anions but exhibited specific sensing behavior toward Hg²⁺ ions as verified by spectral and electrochemical studies.
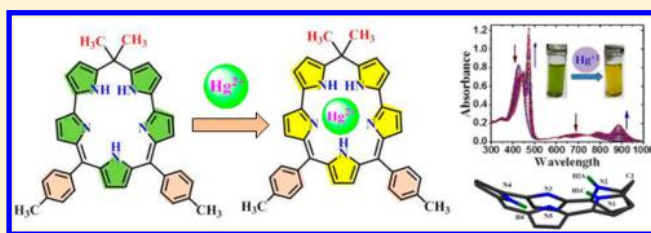
INTRODUCTION

Smaragdyrins[1] and sapphyrins[2] are pentapyrrolic 22π-electron-conjugated macrocycles containing an additional pyrrole compared to tetrapyrrolic porphyrins. Sapphyrins contain four methine bridges and one direct bond, whereas smaragdyrins contain three methine bridges and two direct bonds connecting the five pyrrole rings. Interestingly, sapphyrins **1** are very stable macrocycles and were extensively investigated by Sessler and co-workers for anion/cation complexation studies and also for biomedical applications.[3] However, the chemistry of smaragdyrins was not well explored to a greater extent because of their unstable nature and the lack of proper synthetic methodologies.[1a] Indeed, there are are no reports on *meso*-arylpentaazasmaragdyrin **2** (Chart 1), although one sporadic report is available on β-substituted isosmaragdyrin,[4] which indicates that the synthesis of stable *meso*-arylpentaazasmaragdyrin still remained a challenging problem to solve. The inherent unstable nature of *meso*-arylazasmaragdyrin prevented a study of the properties in detail. In this paper, the synthesis, structure, and properties of stable *meso*-arylcalixazasmaragdyrins **3a/3b** containing five pyrrole rings connected by using two *meso*-sp² carbon atoms, one *meso*-sp³ carbon atom, and two direct bonds are described. We thought the presence of *meso*-sp³ carbon induces conformational flexibility to the macrocycle and allows the macrocycle to be stable. Furthermore, the expanded porphyrin macrocycles have been extensively used for anion-binding studies, but reports on metal-ion-binding studies of the aza-expanded porphyrins are scarce.[5] Because we successfully synthesized the first stable calixazasmaragdyrin **3** having five coordinating nitrogen atoms with three ionizable inner NH

protons, we investigated its cation- and anion- sensing properties. Our studies revealed that calixazasmargadyrin **3** can act as a specific sensor for the Hg²⁺ ion.

RESULTS AND DISCUSSION

The required precursors, 2,2′-(1-methylethylidene)bis(pyrrole) (**4**)[6] and tripyrromethanes **5a/5b**,[7] were synthesized by adopting the literature methods. The calixazasmaragdyrins **3a** and **3b** were prepared by trifluoroacetic acid (TFA) catalyzed condensation of **4** with the appropriate tripyrromethanes **5a/5b** (1:1 ratio) in CH₂Cl₂ followed by oxidation with 2,3-dichloro-5,6-dicyano-1,4-benzoquinone (DDQ; Scheme 1). The progress of the reaction was monitored by thin-layer chromatography (TLC) analysis and absorption spectroscopy. The absorption spectrum of crude reaction mixture showed one main absorption peak at ~420 nm and a broad absorption band at ~690 nm. The crude compounds were subjected twice to basic alumina column chromatography and afforded the desired calixazasmaragdyrins **3a/3b** as green solids in 18−20% yield. The macrocycles **3a** and **3b** are freely soluble in common organic solvents and were characterized by high-resolution mass spectrometry (HR-MS; Figures S1 and S2 in the Supporting Information, SI) and 1D and 2D NMR techniques. The identities of the macrocycles **3a/3b** were confirmed by corresponding molecular ion peaks in mass spectra. The molecular structures of macrocycles **3a/3b** were deduced by using ¹H, ¹H−¹H COSY, and NOESY NMR spectra.

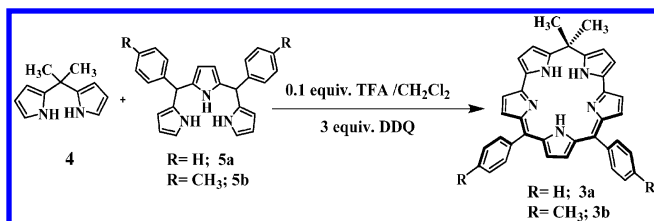**Chart 1. Molecular Structures of Pentaazasapphyrin, Pentaazasmaragdyrin, and Calixazasmaragdyrin**

1	**2**	**3**
Pentaazasapphyrin	Pentaazasmaragdyrin	Calixazasmaragdyrin
(1.1.1.1.0)	(1.1.0.1.0)	(1.1.0./.0)
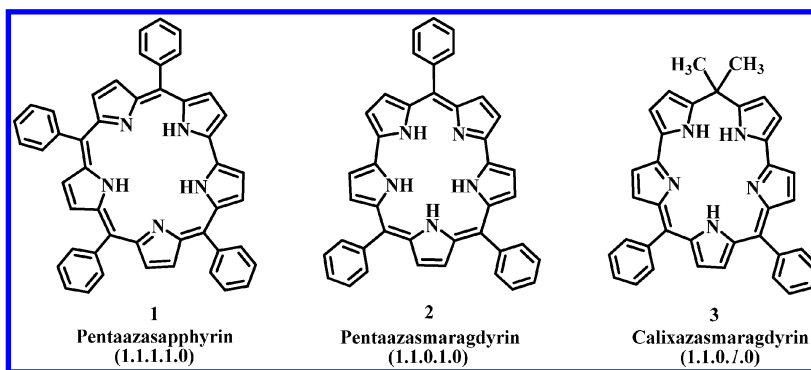
Scheme 1. Synthesis of Calixazasmaragdyrins 3a/3b

The partial ¹H NMR spectrum of calixazasmaragdyrin **3b** is shown in Figure 1a, and selected regions of the ¹H–¹H COSY and NOESY NMR spectra of compound **3b** are shown in parts b and c in Figure 1, respectively. The ¹H NMR spectrum of

calixazasmaragdyrin **3b** showed four doublets at 6.60, 6.48, 6.18, and 5.99 ppm for eight β-pyrrole protons and a singlet at 5.91 ppm for two β-pyrrole protons corresponding to the pyrrole ring, which is trans to sp³ *meso*-carbon (Figure 1a). In ¹H–¹H COSY NMR spectrum of **3b** (Figure 1b), the doublet at 6.60 ppm showed a cross-peak correlation with a doublet resonance at 6.48 ppm, whereas the doublet at 6.18 ppm showed a cross-peak correlation with a doublet resonance at 5.99 ppm. To identify and assign each pyrrole proton, we further carried out NOESY NMR studies of compound **3b**. We first looked at the NOE correlation of the *meso*-methyl group to identify the adjacent e-type pyrrole protons. In the NOESY spectrum (Figure 1c), the singlet at 1.83 ppm corresponding to −CH₃ protons showed a cross-peak correlation with the
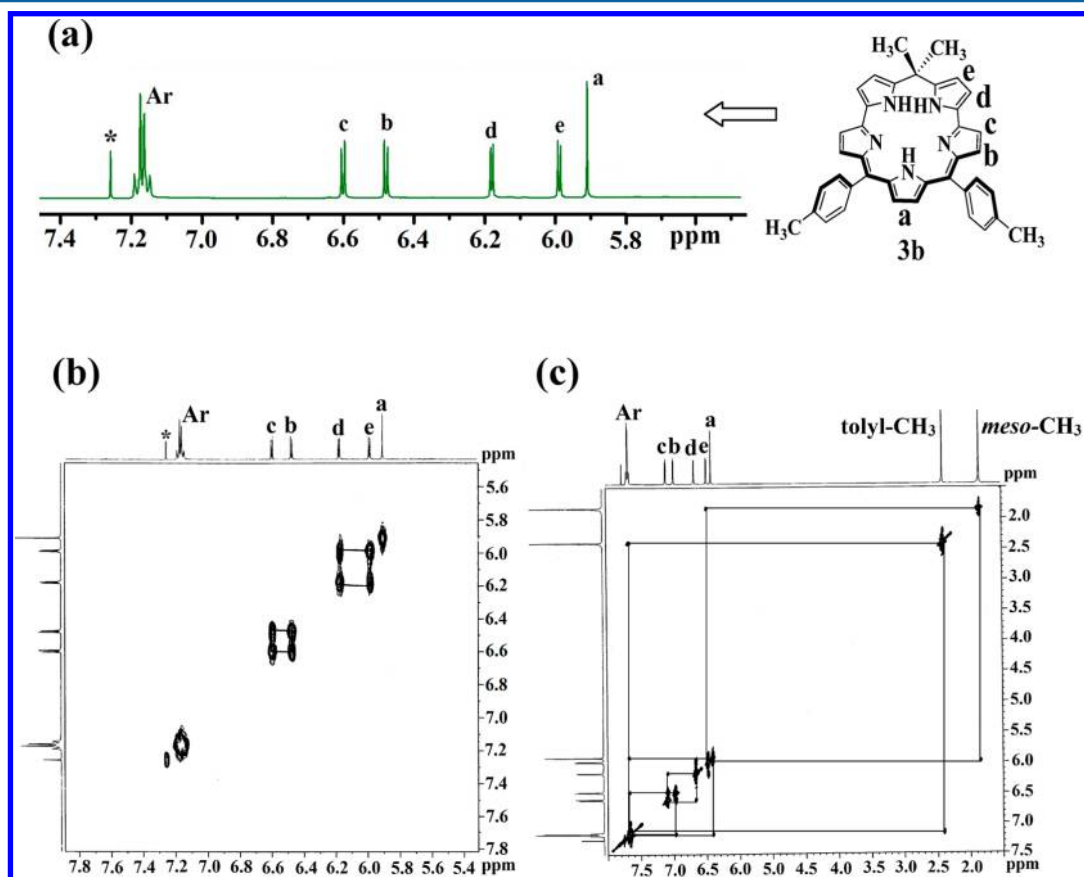

Figure 1. (a) Partial ¹H NMR spectrum of compound **3b** recorded in CDCl₃ (* is the residual solvent peak) at room temperature. (b) Partial ¹H–¹H COSY and (c) NOESY NMR spectra of calixpentaazasmaragdyrin **3b** recorded in CDCl₃ at room temperature.

doublet at 5.99 ppm. This doublet at 5.99 ppm was assigned to e-type pyrrole protons. The doublet at 6.18 ppm was assigned to d-type pyrrole protons based on its correlation with an e-type resonance (Figure 1b). The meta and ortho protons of the *meso*-tolyl group appearing in the ∼7.14−7.19 ppm region showed a correlation with the tolyl −CH₃ proton resonance at 2.39 ppm. The singlet at 5.91 ppm (a-type) and the doublet at 6.48 ppm (b-type) were identified based on their correlations with aryl protons appearing in the ∼7.14−7.19 ppm region. The c-type pyrrole signal at 6.60 ppm was identified from the cross-peak correlation with the b-type pyrrole resonance at 6.48 ppm (Figure 1b). Compound **3a** also showed NMR features similar to those of compound **3b** (Figures S3−S5 in the SI). The resonances due to the inner NH signals in compounds **3a**/**3b** were not observed in the room temperature ¹H NMR spectra, which may be due to rapid tautomerism. Interestingly, in the ¹H NMR spectrum recorded for **3b** at −50 °C, we observed one relatively sharp signal at 12.92 ppm and one broad signal at ∼13.69 ppm corresponding to two types of inner NH protons (Figure S8 in the SI). We also recorded the ¹H NMR spectrum of the protonated species **3b·2H²⁺** at room temperature after the addition of a drop of TFA to the solution of **3b**. We noticed the appearance of three sharp signals in the region of 12−16 ppm due to the inner NH protons along with minor shifts in the resonances of the β-pyrrole and aryl signals. This is due to the restriction of NH tautomerism in the protonated species **3b·2H²⁺** (Figure S9 in the SI).

Crystallographic Characterization of Compound 3b. A good-diffraction-quality violet crystal of compound **3b** was grown via the slow evaporation of *n*-hexane into a CH₂Cl₂ solution of **3b** over a period of 2 days at room temperature. The crystal data are given in Table 1, and bond distances and angles are given in Table 2. The solid-state structure of **3b** given in Figure 2a clearly shows that the pentapyrrolic macrocycle is highly puckered with three inner NH protons.

Table 1. Crystal Data and Data Collection Parameters of Compound 3b

parameter	3b
mol formula	C₃₉H₃₃N₅·H₂O
fw	589.72
cryst syst	monoclinic
space group	$P2_1/c$
temp (K)	100(2)
a (Å)	8.443(2)
b (Å)	16.308(4)
c (Å)	22.317(5)
α (deg)	90
β (deg)	95.490(3)
γ (deg)	90
V (Å³)	3058.7(12)
Z	4
μ (mm⁻¹)	0.08
d_{calcd} (g cm⁻³)	1.276
F(000)	1248
2θ range (deg)	3.02−25.0
indep reflns	5333
R1, wR2 [I > 2σ(I)]	0.050, 0.1189
R1, wR2 (all data)	0.067, 0.1346
GOF	0.92
largest diff peak, hole (e Å⁻³)	0.23,−0.30

Table 2. Selected Bond Lengths and Angles of Compound 3b

bond	bond length (Å)	angle	bond angle (deg)
N1−C1	1.364(2)	C1−C2−C3	107.92(15)
N1−C21	1.374(2)	C38−C2−C39	109.24(16)
N2−C3	1.371(2)	C24−C11−C10	118.25(16)
N2−C6	1.377(2)	C24−C11−C12	117.41(16)
N3−C7	1.339(2)	C31−C16−C15	115.31(15)
N3−C10	1.401(2)	C31−C16−C17	118.47(16)
N4−C12	1.379(2)		
N4−C15	1.379(2)		
N5−C17	1.404(2)		
N5−C20	1.333(2)		
C2−C1	1.525(3)		
C2−C3	1.509(3)		
C2−C38	1.549(3)		
C2−C39	1.527(3)		
C6−C7	1.441(3)		
C20−C21	1.435(3)		

The X-ray structure of **3b** consists of well-separated molecules of calixazasmaragdyrin and a water molecule, which is coordinated to the pyrrole nitrogen atoms of the macrocycle through hydrogen-bonding interactions. To date, the pentaazasmaragdyrin **2** has not been isolated to obtain its crystal structure because of its inherently unstable nature.[1a] However, introducing one sp³ *meso*-carbon in place of the sp² *meso*-carbon resulted in a stable flexible macrocycle of the calixazasmaragdyrin **3b**. The pyrrole rings of the macrocycle **3b** are highly distorted to different magnitudes from the mean plane of the macrocycle comprised of 28 atoms involving five heterocycle rings and three *meso*-carbon atoms. The four pyrrole rings (labeled as 1, 2, 3, and 5) are deviated down to the mean plane, whereas one pyrrole ring (labeled as 4), which is trans to the sp³ *meso*-carbon, is deviated significantly above to the mean plane of the macrocycle (Figure 2c). The pyrrole rings (1 and 2) of the dipyrromethane moiety are markedly deviated from the mean plane by 24° and 44°, respectively, with respect to the mean plane. Furthermore, the two pyrrole rings (1 and 2) of the dipyrromethane moiety make an angle of 68° with each other and significantly deviated from attaining planarity from the mean plane of the macrocycle. The nitrogen atoms N1 and N2 of these two pyrrole rings (1 and 2) are significantly shifted from the 28-atom mean plane and placed above at a distance positioned at 0.45 and 0.72 Å, respectively, above the mean plane. The most deviated pyrrole ring is the one that is opposite to the sp³ *meso*-carbon (pyrrole ring 4). However, the pyrrole nitrogen atom is almost at the mean plane of the macrocycle. The other two pyrrole rings 3 and 5 are almost in the mean plane and show very little deviation. Thus, the maximum deviations were observed in the case of three pyrrole rings (1, 2, and 4) that have the inner NH atoms (Figure 2c). The sp³ *meso*-carbon atom (C2) is deviated significantly from the mean plane (∼1.28 Å), whereas the two sp² *meso*-carbon atoms (C11 and C16) are positioned at almost the mean plane of the macrocycle (Figure 2d). The *meso*-tolyl groups make average dihedral angles of ∼45° with the macrocycle skeleton, indicating that the *meso*-tolyl groups are more coplanar with the smaragdyrin skeleton. Thus, the calixazasmaragdyrin ring of **3b** is highly distorted (Figure 2d). Thus, the presence of both sp² and sp³ carbon atoms in the calixazasmaragdyrin skeleton
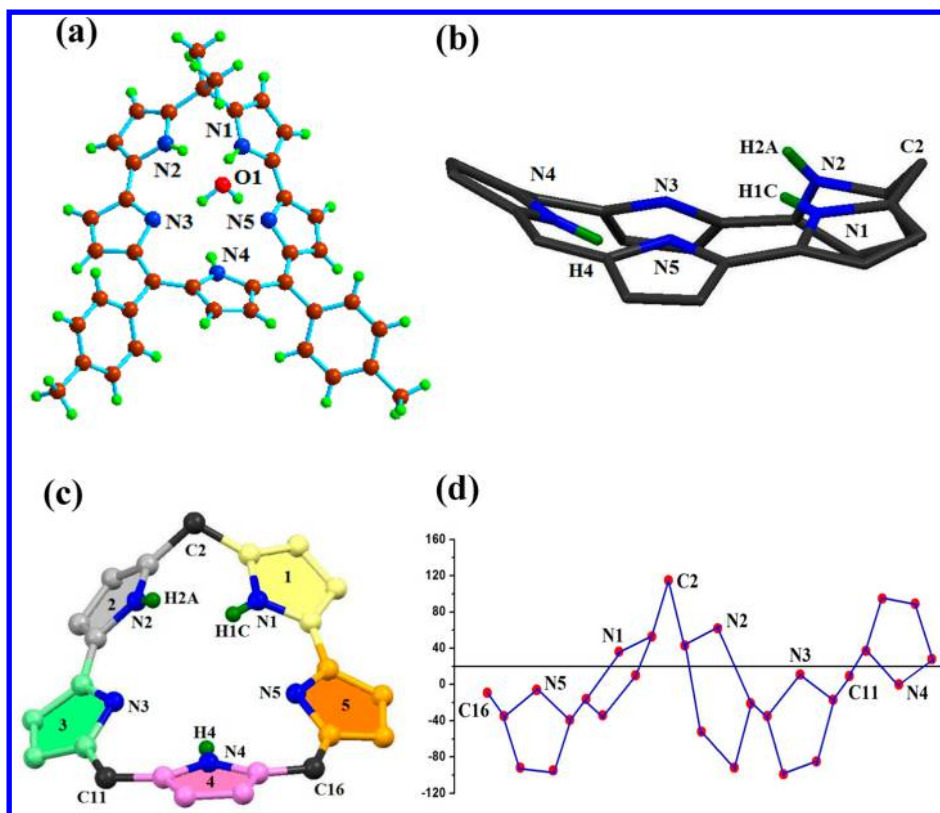
Figure 2. (a) Perspective view of compound **3b**. Thermal ellipsoids are drawn at 50% probability. (b) Side view of compound **3b** (*meso*-tolyl groups and hydrogen atoms are omitted for clarity). (c) Representation of the five pyrrole rings and three *meso*-carbon atoms in compound **3b** (*meso*-tolyl groups and hydrogen atoms are omitted for clarity). (d) Diagram showing out-of-plane displacements (in units of 0.01 Å) of the calixazasmaragdyrin **3b** core atoms from the mean plane consisting of $C_{23}N_5$ atoms.
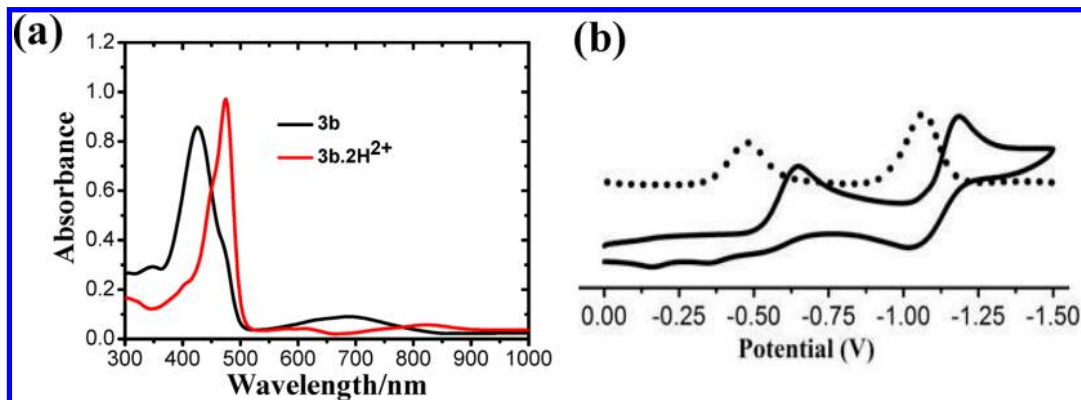

Figure 3. (a) Comparison of the absorption spectra of compounds **3b** (1×10^{-6} M; black) and **3b·2H^{2+}** (1×10^{-6} M; red) recorded in a CHCl$_3$ solvent at room temperature. (b) Reduction waves of cyclic voltamograms along with differential pulse voltammograms (dotted line) of compound **3b** recorded in CH$_2$Cl$_2$ containing 0.1 M TBAP as the supporting electrolyte and a saturated calomel electrode (SCE) as the reference electrode at scan rates of 50 mV s^{-1}.

Table 3. Absorption and Electrochemical Data of Compounds 3a, 3b, 3b·2H^{2+}, and 3b·Hg^{2+}

	absorption data		redox data						
			oxidation (V)				reduction (V)		
compound	Soret band (nm) (log ε)	Q bands (nm) (log ε)	I	II	III	IV	I	II	III
3a	425 (5.93)	686 (4.95)	0.70	0.96	1.42	1.62	−0.24	−0.57	−1.12
3b	425 (5.92)	685 (4.96)	0.71	0.95	1.42	1.62	−0.25	−0.59	−1.11
3b·2H^{2+}	475 (5.99)	821 (4.74)							
3b·Hg^{2+}	470 (6.08)	889 (5.26)							

Figure 4. (a) Absorption spectra of compound **3b** (1×10^{-6} M) in the presence of various metal ions (excess of equivalents) recorded in a CHCl$_3$ solution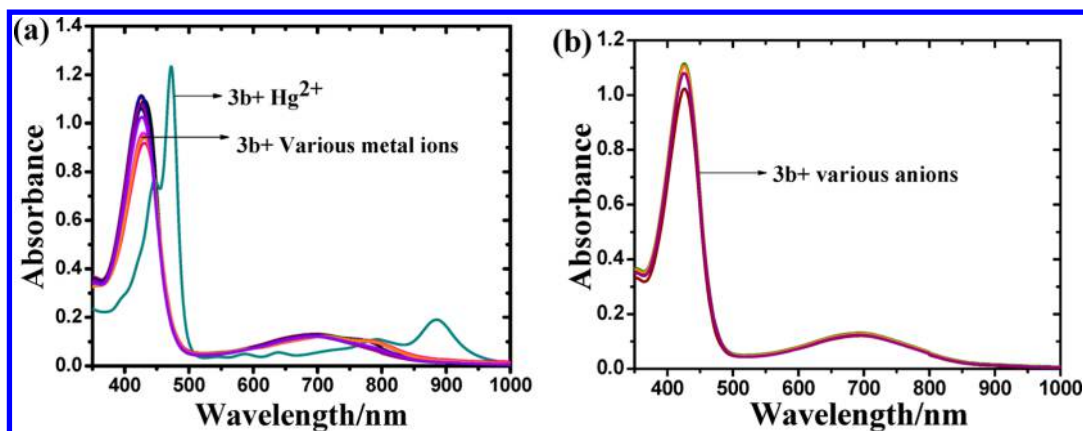. (b) Absorption spectra of compound **3b** (1×10^{-6} M) in the presence of various anions (excess of equivalents) recorded in a CHCl$_3$ solution.
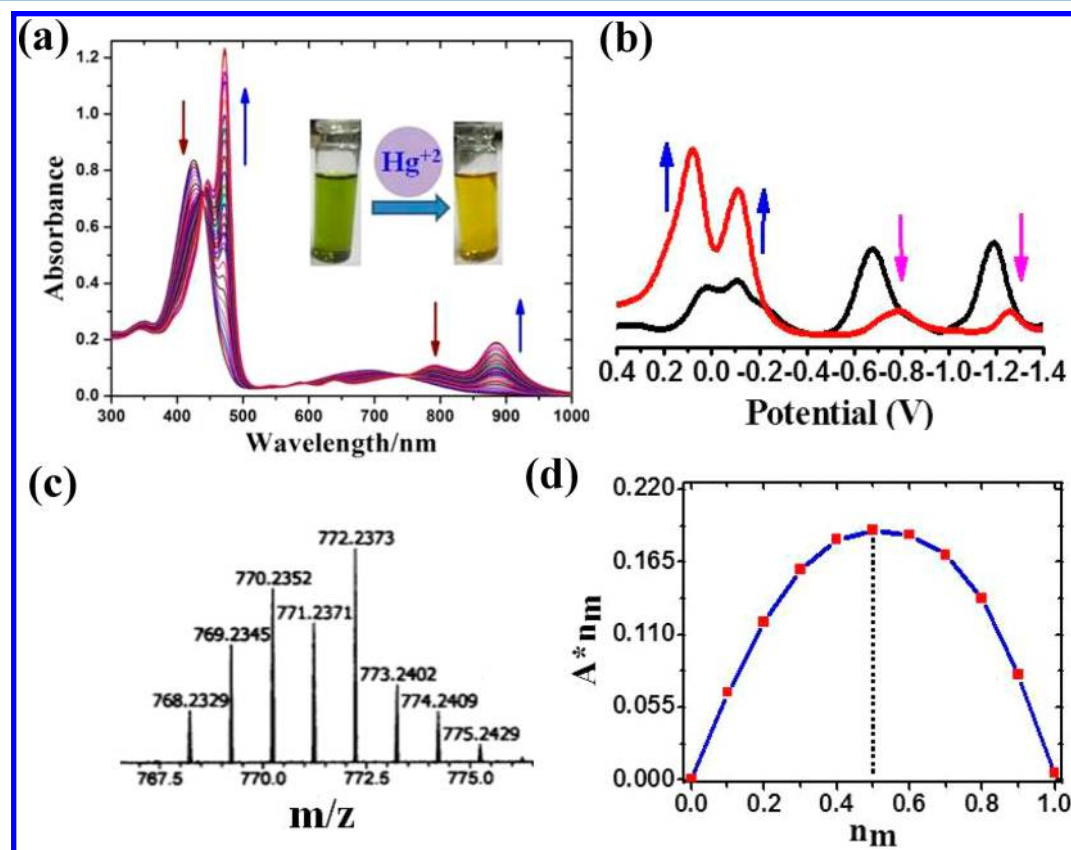

Figure 5. (a) Changes in the absorption spectra of compound **3b** (1×10^{-6} M) upon the systematic addition of Hg^{2+} ion (0−20 equiv) in a CHCl$_3$ solution. The inset shows the color change of compound **3b** to the naked eye upon the addition of Hg^{2+} ion. (b) Square-wave voltammograms of compounds **3b** (black) and **3b** + 10 equiv of Hg^{2+} ion (red) in CH$_2$Cl$_2$ containing 0.1 M TBAP as the supporting electrolyte recorded at a scan rate of 50 mV s^{-1}. (c) Job's plot for the evolution of binding stoichiometry between compound **3b** and Hg^{2+} in a CHCl$_3$ solution, where n_m is mole fraction of the metal ion (Hg^{2+}) added and A is the absorbance. (d) HR-MS spectrum of compound **3b** + Hg^{2+} ion.

makes the system more flexible and attains a boat-shaped structure (Figure 2b).

Absorption and Electrochemical Properties. The absorption and electrochemical properties of calixazasmaragdyrins **3a** and **3b** were investigated. The absorption spectra of **3b** along with its diprotonated form **3b·2H^{2+}** are shown in Figure 3a. The macrocycles **3a** and **3b** showed one strong band at ∼425 nm and one ill-defined broad band at ∼685 nm (Table 3). Upon protonation, the macrocycle **3b·2H^{2+}** showed a red-

shifted sharp band at 475 nm and an ill-defined band at 821 nm. The macrocycles **3a** and **3b** were nonfluorescent. The redox properties of macrocycles **3a**/**3b** were investigated, and the data are included in Table 3. A representative reduction wave of macrocycle **3b** is presented in Figure 3b. The macrocycles **3a** and **3b** showed irreversible oxidations and reductions, indicating that the macrocycles **3a** and **3b** were not stable under redox conditions.

Hg^{II}-Ion-Sensing Studies. Because the macrocycles **3a** and **3b** have five nitrogen atoms with three ionizable hydrogen atoms, we anticipated that calixazasmaragdyrins can bind metal ions easily. We investigated the metal-ion-sensing capability of the calixazasmaragdyrin **3b** with diverse mono-, di-, and trivalent metal ions in a CHCl$_3$ solution. In order to establish the selective metal-ion-binding behavior of **3b**, absorption spectral titrations were carried out in CHCl$_3$ with excess equivalents of different metal perchlorates such as Li$^+$, Na$^+$, K$^+$, Ca^{2+}, Mg^{2+}, Mn^{2+}, Fe^{2+}, Co^{2+}, Ni^{2+}, Cu^{2+}, Zn^{2+}, Cd^{2+}, Hg^{2+}, Cr^{3+}, and Fe^{3+}, and we noticed clear changes in the absorption spectrum of **3b** only upon the addition of Hg^{2+} ion (Figure 4a). The color of the solution also changed markedly from green to yellow upon the addition of Hg^{2+} ion to macrocycle **3b**. Furthermore, we did not observe any significant changes either in absorption maxima or in solution color upon the addition of various anions (tetrabutylammonium salts), indicating that macrocycle **3b** did not show any sensing behavior toward anions (Figure 4b). The absorption spectral titration studies were performed by the addition of increasing amounts of Hg^{2+} ions to a chloroform solution of **3b**, as shown in Figure 5a. The sequential addition of Hg^{2+} ions to a CHCl$_3$ solution of compound **3b** resulted in a decrease of the absorption bands at 425 and 685 nm and the appearance of new bands at 470, 790, and 889 nm with two clear isosbestic points at 616 and 600 nm. This indicates the presence of two species in solution, free base **3b** and the mercury-bound complex **3b·Hg^{2+}** (Table 3). We further followed the interaction of **3b** with Hg^{2+} ion by square-wave voltammetry, and the changes in the redox potentials upon the addition of increasing amounts of Hg^{2+} ions are shown in Figure 5b. The redox waves at −0.20, −0.75, and −1.16 V were decreased in intensity with the simultaneous increase of the redox waves at −0.12 and 0.08 V upon the addition of Hg^{2+} ion, supporting the interaction between Hg^{2+} ion and macrocycle **3b**. Further support for the interaction between **3b** and Hg^{2+} ion was obtained from the molecular ion peak at 772.2373 corresponding to the **3b·Hg^{2+}** complex in the HR-MS spectrum (Figure 5c). Job's plot analyses support the formation of a 1:1 complex between calixazasmaragdyrin **3b** and Hg^{2+} ion, which is in agreement with the HR-MS mass spectrum obtained for the **3b·Hg^{2+}** complex (Figure 5d). The interaction of **3b** with Hg^{2+} ion was evaluated by a Benesi−Hildebrand equation and found to have an association constant of 1.9×10^4 M^{-1}. To establish the binding mode of Hg^{2+} with **3b**, we also carried out density functional theory calculations using the *Gaussian 03* packages[8] (Figures S17−S19 in the SI). The initial model for **3b** was taken from the crystal structure, the complex [**3b·Hg^{2+}**] was optimized using B3LYP/LANL2DZ, and the structure obtained with a stabilization energy of −62.7 kcal mol^{-1} is shown in Figure 6. Our calculations support that Hg^{2+} ion binds with the two pyrrolic immine nitrogen atoms of **3b** that are trans to each other in an almost linear fashion. The optimized structure for [**3b·Hg^{2+}**] reveals that the N−Hg^{2+} distance is ∼2.21 Å and exhibits an N−Hg−N angle of ∼159° (Figure 6). This bond distance is almost in a range similar to that of the reported porphyrin−mercury(II) complexes.[9] However, the bond angle is slightly away from a perfect linear geometry because of the presence of three NH atoms, which causes steric hindrance for Hg^{2+} ion binding to macrocycle **3b**. Furthermore, to establish the involvement of the binding of two immine nitrogen atoms with Hg^{2+} ion in the **3b·Hg^{2+}** complex, we recorded the ^{1}H NMR spectrum of **3b** after the addition of excess equivalents of
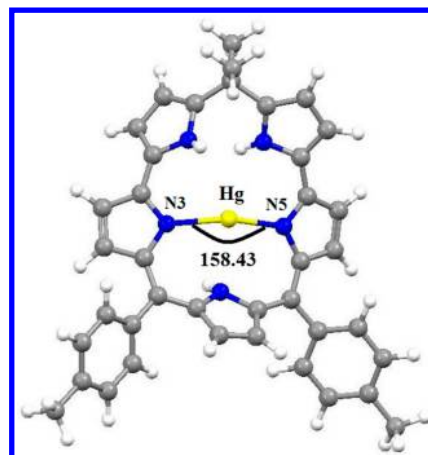

Figure 6. B3LYP/LANL2DZ-optimized structure of complex **3b·Hg^{2+}**.

Hg^{2+} ion at −50 °C. We noted the appearance of two broad signals at 12.84 and 13.76 ppm due to three inner NH protons, which indicates that the three NH protons were intact. This observation supports the binding of the two immine nitrogen atoms of **3b** with Hg^{2+} ion (Figures S12 and S13 in the SI).

Furthermore, we tested the reversibility and reusability of the calixazasmaragdyrin **3b** by carrying out three alternating cycles of UV titration of **3b** with Hg^{2+} followed by washing with H$_2$O or by the addition of a strong chelating agent like ethylenediaminetetraacetic acid (EDTA). After the addition of an excess of HgClO$_4$ salt to the solution of **3b**, we observed the appearance of a sharp absorption band at 472 nm due to formation of the **3b·Hg^{2+}** complex as mentioned above. The **3b·Hg^{2+}** complex solution in CHCl$_3$ was washed thoroughly with H$_2$O, and the CHCl$_3$ layer was separated and dried over anhydrous Na$_2$SO$_4$. The absorption spectrum of the solution showed the disappearance of the absorption band at 472 nm corresponding to the **3b·Hg^{2+}** complex with the appearance of an absorption band at 425 nm corresponding to **3b** (Figure S14 in the SI). The same observation was also found when we repeated this study by treating the **3b·Hg^{2+}** complex solution with a EDTA solution. Being a strong complexing agent, the EDTA ligand forms stable a EDTA−Hg complex by decomplexing **3b·Hg^{2+}** to **3b**, which was confirmed by a clear color change and absorption spectroscopy (Figure S15 in the SI). Thus, from the above experimental observations, it is clear that the calixazasmaragdyrin **3b** can act as a reversible and reusable sensor for Hg^{2+}.

■ CONCLUSIONS

In conclusion, the first stable calixazasmaragdyrins were synthesized by [3 + 2] condensation of dipyrromethane with tripyrrane under mild acid catalyzed conditions. The presence of both sp^2 and sp^3 *meso*-carbon atoms in the macrocycle makes calixazasmaragdyrin a more flexible and stable system. The crystal structure revealed that the macrocycle is highly strained and puckered. Calixazasmaragdyrins showed ill-defined absorption bands because of the disruption of π-electronic conjugation in the macrocyclic skeleton and also exhibited poor redox behavior. The cation- and anion-sensing studies indicate that calixazasmaragdyrins have only a specific sensing affinity toward Hg^{2+} ion in its neutral state over a range of various metal ions and anions. We are currently exploring the coordination chemistry of calixazasmaragdyrins in our laboratory.

EXPERIMENTAL SECTION

Chemicals and Solvents. All of the chemicals such as pyrrole and 2,3-dichloro-5,6-dicyano-1,4-benzoquinone (DDQ) were used as obtained from Aldrich. All other chemicals used for the synthesis were reagent-grade. The solvents like dichloromethane, *n*-hexane, and chloroform were purified and distilled by standard procedures before use. Silica gel and basic alumina used for column chromatography have been obtained from Sisco Research Laboratories, India. Tetrabutylammonium perchlorate (TBAP) was purchased from Fluka. All NMR solvents were bought from Aldrich. The known compounds 2,2′-(1-methylethylidene)bis(pyrrole) (**4**),[6] 5,10-diphenyltripyrromethane (**5a**),[7] and 5,10-di(*p*-tolyl)tripyrromethane (**5b**)[7] were prepared according to the published procedures.

Instrumentation. The ^{1}H and ^{13}C NMR (δ in parts per million) spectra were recorded by using Bruker AVANCE III 400 and 500 MHz spectrometers. Tetramethylsilane was used as an internal reference for recording ^{1}H NMR spectra (residual proton; δ = 7.26 ppm) in CDCl$_3$. The HR-MS spectra were recorded by a Q-TOF micromass spectrometer based on the electrospray ionization method. Cyclic, differential pulse, and square-wave voltammetry experiments were carried out in a BAS electrochemical system, by using glassy carbon as the working electrode, platinum wire as the auxiliary electrode, and saturated calomel as the reference electrode.

Collection and Reduction of X-ray Data. X-ray data for structure analysis were collected on a Rigaku Saturn 724 diffractometer, which was attached with a low-temperature accessory. The diffractometer was accompanied by a CCD area detector and operated with graphite-monochromated Mo Kα radiation (λ_α = 0.71073 Å) by an ω-scan technique. The data were collected at 100 K. With the aid of initial scans obtained for the crystal, we assigned the preliminary unit cell parameters and the required number of frames for data collection. The obtained data were integrated using *CrystalClear-SM Expert 2.1 b24* software. The structure was solved by direct methods and refined using different software packages like *SHELXL-97*,[10] *SIR-92*,[11] and *WINGX*.[12] All non-hydrogen atoms were refined anisotropically, and the hydrogen atoms were fixed at the calculated position using the riding model.

CCDC 1035396 (for **3b**) contains supplementary crystallographic data and is available free of cost from the Cambridge Crystallographic Data Centre via www.ccdc.cam.ac.uk/data_request/cif.

Metal-Ion-Binding Studies. All of the metal ion and anion salts used for titration are their perchlorate and tetrabutylammonium salts, respectively. The absorption measurements were performed using the diluted stock solution of **3b** (1×10^{-6} M) after the addition of requisite amounts of different metal ions or anions. The association constant of the **3b·Hg^{2+}** complex formed in the solution has been calculated by using the standard Benesi–Hildebrand equation.[13]

General Synthesis of Compounds 3a/3b. The condensation of tripyrromethanes **5a/5b** (1.26 mmol) and dipyrromethane **4** (1.26 mmol) in 500 mL of dry dichloromethane was carried out in the presence of 0.1 equiv of TFA as a catalyst under an inert atmosphere at room temperature for 1.5 h. The sample of 3 equiv of DDQ was added, and the reaction mixture was stirred in open air for an additional 1.5 h. The TLC analysis of the reaction mixture clearly showed the appearance of a minor yellowish spot, followed by a major green spot. The solvent was evaporated, and the crude compound was subjected twice to basic column chromatography. The desired calixazasmaragdyrin was eluted as a green band by using petroleum ether/dichloromethane (60:40) and afforded a green solid of pure **3a/3b** in 20–22% yield.

Compound 3a. Yield: 20% (135 mg). ^{1}H NMR (400 MHz, CDCl$_3$, 25 °C): δ 7.42–7.28 (m, 10H, Ar), 6.62 (d, 2H, J = 4.6 Hz, c-type β-pyrrole), 6.46 (d, 2H, J = 4.6 Hz, b-type β-pyrrole), 6.22 (d, 2H, J = 3.7 Hz, d-type β-pyrrole), 6.02 (d, 2H, J = 3.7 Hz, e-type β-pyrrole), 5.87 (s, 2H, a-type β-pyrrole), 1.83 (s, 6H, CH$_3$). ^{13}C NMR (400 MHz, CDCl$_3$, 25 °C): δ 139.53, 137.90, 131.58, 131.55, 128.85, 127.75, 125.21, 123.51, 111.34, 111.22, 107.30, 107.23, 36.37, 29.23. UV–vis [λ_{max} nm (log ε); CH$_2$Cl$_2$]: 425 (5.86), 686 (4.38). HR-MS. Calcd for C$_{37}$H$_{30}$N$_5$ [(M + H)$^+$]: *m/z* 544.2505. Obsd: *m/z* 544.2496.

Anal. Calcd for C$_{37}$H$_{29}$N$_5$: C, 81.74; H, 5.38; N, 12.88. Found: C, 81.72; H, 5.34; N, 12.89.

Compound 3b. Yield: 22% (158 mg). ^{1}H NMR (400 MHz, CDCl$_3$, 25 °C): δ 7.19–7.14 (m, 8H, Ar), 6.60 (d, 2H, J = 4.9 Hz, c-type β-pyrrole), 6.48 (d, 2H, J = 4.0 Hz, b-type β-pyrrole), 6.18 (d, 2H, J = 4.9 Hz, d-type β-pyrrole), 5.99 (d, 2H, J = 4.0 Hz, e-type β-pyrrole), 5.91 (s, 2H, a-type β-pyrrole), 2.39 (s, 6H, CH$_3$ tolyl), 1.83 (s, 6H, CH$_3$). ^{13}C NMR (400 MHz, CDCl$_3$, 25 °C): δ 175.41, 162.43, 153.83, 152.81, 140.30, 139.02, 137.91, 136.60, 135.91, 131.60, 128.39, 127.74, 124.98, 123.40, 110.61, 106.88, 36.27, 29.02, 21.47. UV–vis [λ_{max} nm (log ε); CH$_2$Cl$_2$]: 425 (5.91), 685 (4.97). HR-MS. Calcd for C$_{39}$H$_{34}$N$_5$ [(M + H)$^+$]: *m/z* 572.2807. Obsd: *m/z* 572.2809. Calcd for C$_{39}$H$_{33}$N$_5$: C, 81.93; H, 5.82; N, 12.25. Found: C, 81.94; H, 5.84; N, 12.30.

ASSOCIATED CONTENT

⑤ Supporting Information

X-ray crystallographic data in CIF format and characterization data for all new compounds. This material is available free of charge via the Internet at http://pubs.acs.org.

AUTHOR INFORMATION

Corresponding Author

*E-mail: ravikanth@chem.iitb.ac.in.

Notes

The authors declare no competing financial interest.

REFERENCES

(1) (a) Pareek, Y.; Ravikanth, M.; Chandrashekar, T. K. *Acc. Chem. Res.* **2012**, *45*, 1801–1816. (b) Narayanan, S. J.; Sridevi, B.; Chandrashekar, T. K. *Org. Lett.* **1999**, *4*, 587–590. (c) Rajeswara Rao, M.; Ravikanth, M. *J. Org. Chem.* **2011**, *76*, 3582–3587. (d) Kalita, H.; Lee, W.-Z.; Ravikanth, M. *Dalton Trans.* **2013**, *42*, 14537–14544. (e) Kalita, H.; Lee, W.-Z.; Ravikanth, M. *J. Org. Chem.* **2013**, *78*, 6285–6290.

(2) (a) Roznyatovskiy, V. V.; Lee, C. H.; Sessler, J. L. *Chem. Soc. Rev.* **2013**, *42*, 1921–1933. (b) Sessler, J. L.; Tomat, E. *Acc. Chem. Res.* **2007**, *40*, 371–379.

(3) (a) Sessler, J. L.; Cyr, M.; Lynch, V.; McGhee, E.; Ibers, J. A. *J. Am. Chem. Soc.* **1990**, *112*, 2810–2813. (b) Sessler, J. L.; Cyr, M. J.; Burrell, A. K. *Tetrahedron* **1992**, *48*, 9661–9672. (c) Lisowski, J.; Sessler, J. L.; Lynch, V. *Inorg. Chem.* **1995**, *34*, 3567–3572. (d) Furuta, H.; Cyr, M. J.; Sessler, J. L. *J. Am. Chem. Soc.* **1991**, *113*, 6677–6678. (e) Shinoya, M.; Furuta, H.; Lynch, V.; Haniman, A.; Sessler, J. L. *J. Am. Chem. Soc.* **1992**, *114*, 5714–5722. (f) Král, V.; Sessler, J. L.; Furuta, H. *J. Am. Chem. Soc.* **1992**, *114*, 8704–8705.

(4) Sessler, J. L.; Davis, J. M.; Lynch, V. *J. Org. Chem.* **1998**, *63*, 7062–7065.

(5) (a) Wu, D.; Descalzo, A. B.; Weik, F.; Emmerling, F.; Shen, Z.; You, X.-Z.; Rurack, K. *Angew. Chem., Int. Ed.* **2008**, *47*, 193–197. (b) Zhu, X.-J.; Fu, S.-T.; Wong, W.-K.; Guo, J.-P.; Wong, W.-Y. *Angew. Chem., Int. Ed.* **2006**, *45*, 3150–3154.

(6) Littler, B. J.; Miller, M. A.; Hung, C.-H.; Wagner, R. W.; O'Shea, D. F.; Boyle, P. D.; Lindsey, J. S. *J. Org. Chem.* **1999**, *64*, 1391–1396.

(7) Ka, W.-J.; Lee, H. C. *Tetrahedron Lett.* **2000**, *41*, 4609–4613.

(8) Pople, J. A.; et al. *Gaussian 03*, revision C.02; Gaussian, Inc.: Wallingford, CT, 2004.

(9) Lemon, C. M.; Brothers, P. J.; Boitrel, B. *Dalton Trans.* **2011**, *40*, 6591–6609.

(10) Sheldrick, G. M. *Acta Crystallogr.* **2008**, *A64*, 112–122.

(11) Altomare, A.; Cascarano, G.; Giacovazzo, C.; Gualardi, A. *J. Appl. Crystallogr.* **1993**, *26*, 343–350.

(12) Farrugia, L. J. *J. Appl. Crystallogr.* **1999**, *32*, 837−838.

(13) (a) Benesi, H. A.; Hildebrand, J. H. *J. Am. Chem. Soc.* **1992**, *114*, 5714−5722. (b) Liu, Z.; Jiang, L.; Liang, Z.; Gao, Y. *Tetrahedron* **2006**, *62*, 3214−3220. (c) Valeur, B.; Pouget, J.; Bourson, J.; Kaschke, M. *J. Phys. Chem.* **1992**, *96*, 6545−6549.